IEEE Access
Multidisciplinary | Rapid Review | Open Access Journal

Received July 23, 2019, accepted September 3, 2019, date of publication September 11, 2019,
date of current version September 19, 2019.

Digital Object Identifier 10.1109/ACCESS.2019.2940524

Design and Performance Evaluation of a Modular Linear Induction Machine for Rotating Electronic Billboard

NOMAN BALOCH[1], CHA-SEUNG JUN[2], AND BYUNG-IL KWON[1], (Senior Member, IEEE)
[1]Department of Electronic Systems Engineering, Hanyang University, Ansan 15588, South Korea
[2]LG Electronics Gasan Research and Development Campus, Geumcheon-gu 08592G, South Korea

Corresponding author: Byung-Il Kwon (bikwon@hanyang.ac.kr)

This work was supported in part by the BK21PLUS Program through the National Research Foundation of Korea within the Ministry of Education, and in part by the National Research Foundation of Korea (NRF) Grant funded by the Korean Government, Ministry of Science, under Grant NRF-2017R1A2B4007697.

ABSTRACT This paper proposes a rotating electronic billboard (REB) to save the cost of space required for its installation and a modular linear induction machine (M-LIM) to rotate the proposed REB. REBs are generally installed in public places such as subways and airports to display the advertisements. The proposed REB can be installed around a pillar since it is hollow inside, hence, no additional space is required which limits the cost of the space required for REBs. The proposed M-LIM for rotating the proposed REB has a short straight primary and a ring-shaped secondary. The secondary is installed on top of the light emitting diode (LED) display bars such that when secondary rotates, LED bars rotate along with it. To confirm the suitability of the M-LIM in proposed REB, an M-LIM is designed, and the initial results are examined using three-dimensional finite element analysis (3-D FEA) to consider the 3-D effects in the proposed design. A prototype of the proposed M-LIM along with the proposed REB is manufactured and their collective performance is evaluated experimentally. The results show good agreement with the simulation.

INDEX TERMS Light emitting diode bars, modular linear induction machine, rotating electronic billboard, rectangular electronic billboard, ring-shaped secondary, segmented linear induction machine, short primary.

I. INTRODUCTION

Linear induction machines (LIMs) have been receiving considerable research attention in recent years owing to their simplicity, low production cost, decreased energy loss, adjustable mechanism, and robust structure which make them highly reliable [1]. LIMs also exhibit low noise and vibration, better reliability, better efficiency, and low maintenance cost compared to their rotary counterparts [2].Owing to these merits LIMs have been investigated thoroughly according to various applications. LIMs have different structures such as single-sided (single stator) [3], ladder-type single-sided [4], double stator [5], tubular [6], transverse flux [7], arc type [8], and disc-type [9]. A single-stator LIM has many merits such as simple structure, ease of maintenance and low environmental impact.

The design of LIM has been contemplated as an issue of synthesis similar to any other machine design and has been discussed in the literature [10]–[14]. The optimum design of LIM has been studied with different objective functions. The efficiency and power factor of LIM has been improved through design optimization in [13]. Furthermore, [14] presented the influence of different parameters of LIM on its efficiency, power factor and end effect. The effect of different design variables such as number of poles, slot width, stack length and secondary Aluminum thickness has been discussed in [15]. The finite element method (FEM) has also been used for the design of LIM [16]. LIMs have been designed and analyzed for specific requirements [17], [18]. [17] designed a LIM for laboratory experiments, and [18] designed and analyzed especially LIM for railways.

Furthermore, LIMs have proved to be effective in linear metro systems, reducing the cross-sectional area of the tunnels by 40% and the construction cost by 20% [19]. Inspired by this impressive performance, the linear metro in China (Lines No. 4 and No. 5) and the Tokyo subway line in Japan (Line No. L2 (Oedo line)) have adopted LIMs for their linear

The associate editor coordinating the review of this manuscript and approving it for publication was Alfeu J. Sguarezi Filho.

metro systems [20]. LIMs have also been proposed and analyzed for magnetic levitation (Maglev) [21]–[23], whereby they exhibit high speed and low noise operation.

Despite the use of LIMs in a variety of applications, there has hardly been a study on their use in Rotating electronic billboards (REBs). REBs which can be viewed from 360°, are now a days installed in public places such as subways and airports to display advertisements.

This paper proposes a REB that have LED bars distributed all around the rotating screen but is hollow inside. Hence, it can be installed around pillars which limits the required space for installing REBs. Also, the cost of the space required for installing REB is reduced. To rotate the REB, a single-sided LIM with a short primary and a ring-shaped secondary is proposed which is henceforth referred as modular-LIM (M-LIM). The power required to rotate the display screen is adjusted by varying the number of primary modules according to the size of REB. The design of M-LIM along with the constraints and limitations that are specific to this application are explained in detail in this paper. A prototype of the proposed REB and proposed M-LIM is fabricated. The experimental results confirm that the desired performance is achieved.

II. EXISTING RECTANGULAR AND ROTATING ELECTRONIC BILLBOARD

In recent years, there has been a rapid increase in outdoor advertisements, especially by means of billboards. A few distinctive features of billboard advertisements are as below [24]:

- High rate of exposure to public.
- Round-the-clock advertisement.
- Low production cost.
- Placement of billboards at strategic locations

1) RECTANGULAR ELECTRONIC BILLBOARDS

Rectangular electronic billboards are usually installed around the pillars/columns in public places such as bus stops, subways, and airports, as shown in Fig. 1 [25]; however, they often require a larger installation space. To facilitate view from all directions, display screens are installed on all the four sides of column due to which it becomes more cost expensive. Moreover, the viewing angle is also a concern as it is limited to 160 degrees.

An electronic billboard patented in United States uses a display screen with an electronic circuitry for advertisement purposes [26]. The advertisements are displayed round-the-clock in the form of pictures or short videos. Recently, the design of electronic billboards has evolved rapidly. Previously, liquid-crystal displays (LCDs) were often used which are cheap but have low efficiency and low display quality; however, nowadays, bright LEDs are preferred owing to their ability to display clear colorful high-quality images.

2) ROTATING ELECTRONIC BILLBOARDS (REBS)

REBs, which can be viewed from 360°, are especially preferred for outdoor advertisements. The REB shown

FIGURE 1. Rectangular electronic billboard [25].

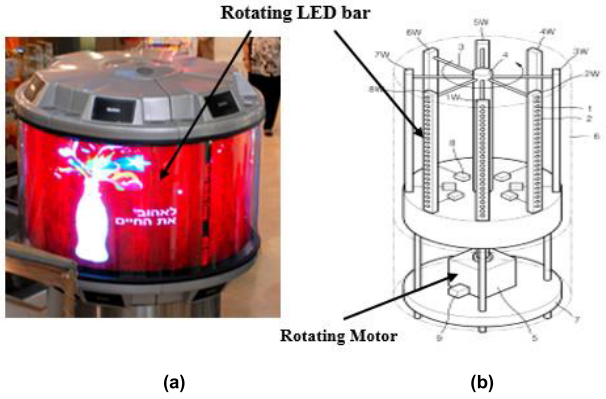

FIGURE 2. Rotating electronic billboard. (a) Existing rotating electronic billboards. (b) Schematic view of REB [27].

in Fig. 2(a) [27] uses thin rectangular LED bars placed in a circular manner, instead of the large-and-thick rectangular LED bars used in rectangular electronic billboards. This makes the REBs cost effective. The LED bars need to rotate at a pre-defined speed so that the human eyes can perceive the images in a normal manner from all directions. For this purpose, a rotary machine is installed inside the REB to rotate the LED bars at a constant speed. The schematic view of a REB is shown in Fig. 2(b). However, the key disadvantage of such a rotary machine placed inside the REB arises when the size of REB changes. In such a case, the motor size and power must be changed, and therefore, the motor must be redesigned for different sizes of REB. Another major disadvantage of such a system is that REBs of this kind require separate space for installation because they cannot be installed around the pillars in the way it is implemented for rectangular electronic billboards. This is because the rotary machine along with the electronic circuitry is installed inside the REB thereby leaving no space of the pillar. Fig. 3 shows a belt-driven REB that has a rotating motor installed outside the REB [28].

In such a system, the motor is installed in a separate space away from the REB, and the LED bars are rotated with the help of a bearing and a belt. Thus, the belt-driven system has a few disadvantages. First, they have an additional

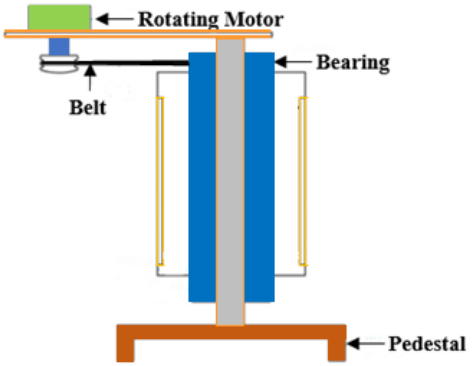

FIGURE 3. Magnet Belt-driven REB [28].

loss due to belt, and it requires extra space for the rotating mechanism. Therefore, the cost of space for installing REB is also increased. Second, the connecting mechanism, which comprises of the belt and pulley, complicates the REB system resulting in low reliability. Third, the machine needs to be redesigned for different sizes of REB according to the power requirements. It is noteworthy that the proposed LIM provides the solutions to overcome all the aforementioned limitations. It should be noted that the rotary motor used for such application will have higher power density and higher efficiency. However, the main target of the research is to propose a REB which can be installed around pillars which will limit the cost of the space required for installing REBs. In addition, other feasible configurations could be used for such a hollow REB with a ring shaped stator and a ring shaped rotor; however, the machine would have to redesigned for different size of REBs.

III. PROPOSED REB AND PROPOSED MODULAR LIM

A. PROPOSED ROTATING ELECTRONIC BILLBOARD

In this paper, a new configuration of REB is proposed. A 3-D view of the proposed REB is shown in Fig. 4. It mainly comprises of top lid, modular LIM, and LED bars. The electronic circuitry is installed just behind the LED bars. The electric power to the LED bars is provided through brushes and slip rings. The brushes are installed just below the top lid and the slip rings are installed around the complete REB. Moreover, the primary modules are attached to the top lid of REB. With an appropriate airgap between primary and secondary, the ring-shaped secondary consisting of an aluminum plate and back iron is installed. Moreover, the LED bars are attached to the secondary back iron. It should be noted that REB is hollow internally. The key advantage of such systems is that they can be installed around a pillar, and they do not require separate space unlike the conventional REBs, which is the main target of this paper. Hence, cost of the space required for installing REBs is also limited compared to conventional REBs. Moreover, the motor that drives the REB is installed on top of the LED bars as shown in Fig. 5; and thus, the belt-driven mechanism is avoided. The main parameters of the complete REB and the basic M-LIM are shown in Table 1.

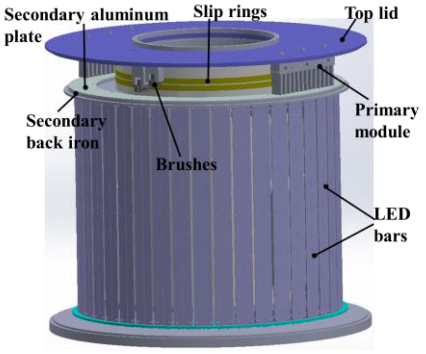

FIGURE 4. 3-D view of proposed configuration.

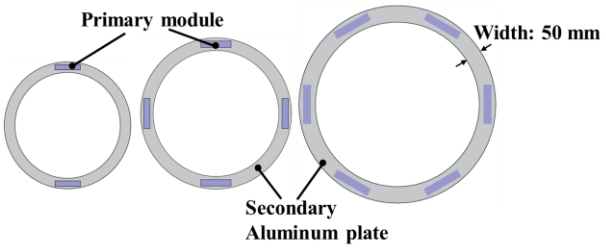

FIGURE 5. Top view of M-LIM for the different LED sizes of REB.

TABLE 1. Main parameters of rotating electronic billboard.

	Item	Unit	Value
Rotating Electronic Billboard	REB outside diameter	mm	300
	REB inside diameter	mm	250
	REB width	mm	50
	REB height	mm	500
	REB weight	kg	9.2
	Frame rate	Hz	60*3
	Resolution	pixels	384
	Bit processing	bits	120
	LED bars	-	40
Linear Induction Machine (single primary)	Current density	A/mm^2	4
	Rated current	A	0.65
	Rated voltage	V	254
	Rotating speed	rpm	180

B. PROPOSED MODULAR LIM

The design procedure used for the M-LIM is shown in Fig. 6. First, the desired thrust force, speed, and power of the machine are determined. The power of the machine is decided based on the size, weight, and inertia of the REB. The weight of the rotating part is determined based on equipment which will be installed within the REB. The important equipment that are installed inside the REB are rectangular LED bars, electronic circuitry behind the bars, ring-shaped aluminum (secondary of induction machine) and the speed sensor installed behind the LED bars. Depending on the inertia, an estimated required force to rotate such a REB at

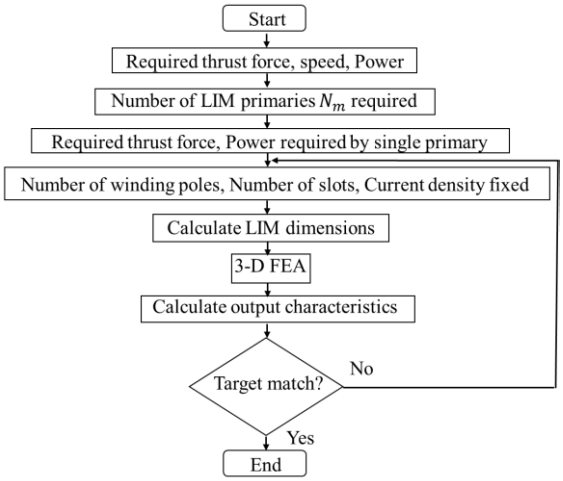

FIGURE 6. Design flow chart for Modular LIM.

our desired speed is determined. The rotating speed of the REB is decided based on the frequency of rotating electronic images within the rectangular bars. The frequency of electronic image is decided based on the number of rectangular LED bars. If the electronic image frequency is kept high, then the required number of LED bars is reduced which will affect the overall cost of the REB. In the designed REB system, the electronic frequency was decided to be 180 Hz and hence to see a stable image on the rotating LEB bars, the REB must rotate at 180 rpm in opposite direction of rotating images. Hence, rotating speed is decided. Based on the size (circumference) of the REB and the power required, the total number of M-LIM primary modules (N_m) is determined. The total power is divided by N_m, and the power that needs to be delivered by each primary module is determined. A video frame rate of 180 Hz is adopted for the LED bars. In order to see a stable image on the display screen, the REB must rotate at 180 rpm in the direction opposite to the video/image. Based on the required rotating speed of LED bars, the linear speed of the proposed machine is calculated. Considering, the outer and inner diameters of the REB, the rated linear speed of the machine is estimated to be 5.2 m/s. Once the above parameters are determined, then the number of slots, winding poles, and current density are decided. The number of slots and poles effect the phase unbalance of the machine. Low poles increase the phase unbalance. Hence, 24 slot and 4 poles were decided keeping in view the previous discussed reason. The current density is selected as 5 A/mm^2, considering the natural cooling required for the proposed machine. This is because the proposed REB system will be installed in public places commercially. Hence, to avoid complications, natural cooling will be used therefore, current density was decided not to be kept greater than 5 A/mm^2. The length of the primary is very important and is set as a design constraint. If the length of the primary is increased beyond a fixed point, some parts of primary will be outside the secondary which will generate leakage flux. The length of primary was

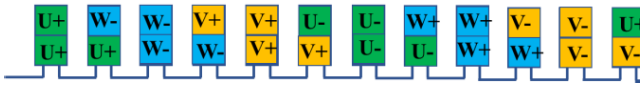

FIGURE 7. Winding layout of the analysis model for 24 slots; only half (12 slots) shown, considering symmetric condition.

finally determined to be 183 mm. The thickness of REB is an important deciding factor for determining the length of the primary. This is because the ends of the primary should not exceed the width of the secondary, that is installed above the REB. The thickness of the REB is determined based on the equipment installed inside the REBs. The equipment installed inside the REB is LED bars, electronic circuitry to run these LED bars and speed sensor. This width was found to be 50 mm. The secondary aluminum width was kept according to this thickness hence, it was determined to be 50 mm. The primary dimensions such as tooth width and slot width are determined initially using analytical calculations and then finalized based on FEA results. Most of the remaining dimensions are finalized based on FEM results. When the output of the LIM is matched with the target, LIM design algorithm is ended. Fig. 7 shows the winding layout of the 24-slot 4-pole model; however, the figure only shows 12 slots, considering the symmetric arrangement of the remaining 12 slots. The design algorithm is followed, and the main parameters of the primary and secondary of the LIM are calculated. All the equations used in the design of M-LIM are taken from reference [29]. The dimensions of the primary are finalized after repetitive simulations, considering the constraints of design and the required thrust force. 3-D FEA was used for the design of the proposed M-LIM to consider the 3-D effects as elaborated further in the subsequent sections.

IV. PERFORMANCE OF PROPOSED MODULAR LIM

A. 3-D FINITE ELEMENT ANALYSIS

3-D FEA is performed for examining the performance of the designed machine. A commercially available FEM software, namely "Ansys Maxwell version 19" is used for the analysis of the proposed M-LIM. The mesh size is kept small, and the machine is simulated for 30 electrical cycles to obtain stable results. The 3-D model of the machine is shown in Fig. 8. The main parameters of the designed M-LIM are shown in Table 2.

The M-LIM is simulated using a voltage source with a frequency of 60 Hz initially. Subsequently, the frequency of the machine is increased in increments of 5 Hz to determine the effect of the slip on the performance. The desired thrust force is obtained at 65 Hz. The line-to-line input voltages using 3-D FEA with a 65 Hz frequency are shown in Fig. 9.

Each phase has a line-to-line rms value of 440 V. The corresponding currents in 3-D FEA are shown in Fig. 10. The obtained currents are found to be unbalanced. The main reason for this is the end effect and asymmetric windings [32]. The asymmetric winding is due to the linear nature of the machine. The phase unbalance of LIM has been discussed in

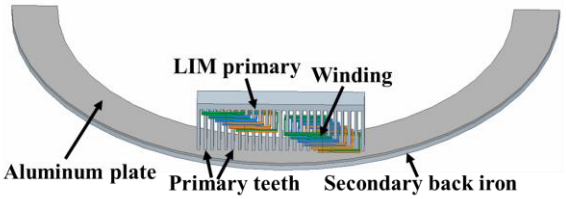

FIGURE 8. 3-D FEA model of LIM.

TABLE 2. Main parameters of M-LIM.

Item	Unit	Value
Primary stator length	mm	183
Primary height	mm	61
Stack length	mm	25
Slot height	mm	53
Slot width	mm	4.5
Teeth width	mm	3
Aluminum thickness	mm	3
Secondary back iron height	mm	6
Air gap	mm	4
Number of primaries	-	2
Number of slots	-	24
Number of poles	-	4
Number of turns/phase	-	2000
Conductor diameter (AWG)	mm	0.4547(25)
Fill factor	%	34

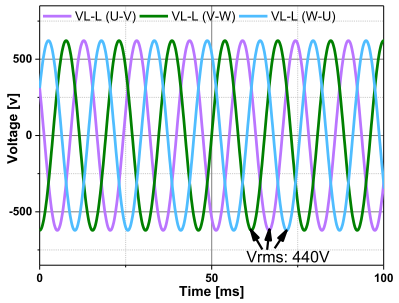

FIGURE 9. Simulated line to line voltages.

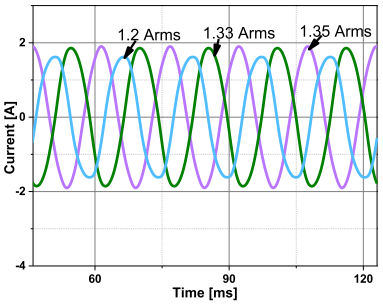

FIGURE 10. Simulated currents.

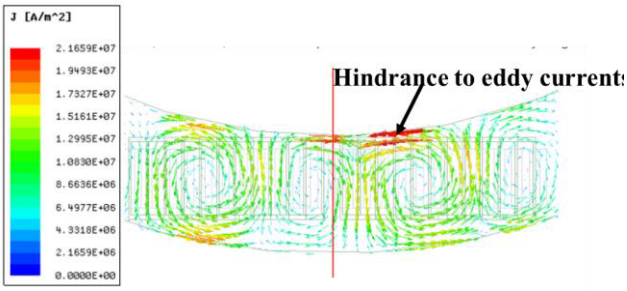

FIGURE 11. Eddy currents induced in secondary aluminum plate.

detail in [30], where it is pointed out that the phase unbalance decreases with an increasing number of poles. Moreover, the phase unbalance also decreases as the length of the primary increases. However, for the proposed REB, the length of the primary cannot be increased beyond a specific value as it would otherwise result in a misalignment between the primary and secondary (edges of the primary would be outside the secondary aluminum plate). Two important characteristics of the designed machine are:

1) The stack length of the primary of the machine was finally decided to be 25 mm, which is small. The stack length of the primary is a constraint and cannot be increased beyond the REB width. If the stack length of the primary is increased beyond a fixed point, some parts of primary will not be exactly on top of secondary and hence, it will produce leakage flux. To avoid this issue and to keep primary always on top of secondary, the stack length was fixed to be 25mm. Owing to this short stack length, the end winding has a significant impact on the output of the machine.

2) The limited width of the ring-shaped secondary can only be modeled in 3-D (Fig. 5). The eddy currents induced on the aluminum plate are shown in Fig. 11. It can be seen that the induced eddy currents are facing a hindrance at the edges of the aluminum plate due to the its limited width. Increasing this width can improve the performance of the machine. Since the ring-shaped secondary rotates, the torque of the machine is calculated in 3-D FEM instead of the thrust force. The effect of increasing the aluminum width on torque is shown in Fig. 12. It can be observed that the torque of the machine increases with the aluminum width. However, the width of the aluminum plate cannot be increased beyond the width of REB because it would otherwise increase the overall size of REB, which is not desirable. The effect of increasing the width of aluminum on torque ripple of the machine is also shown in Fig. 12. The torque ripple of the machine is high. This is due to the limited width of the aluminum, which is a design constraint. It can be observed that torque ripple decreases significantly as the width increases. The torque of the designed LIM at 65 Hz is shown in Fig. 13.

The average torque of the machine is 0.9 Nm, which is the required torque to rotate the machine at 180 rpm. However, the torque ripple of the machine is high. Nonetheless a smooth operation was found in the experiment. It is estimated that the ripple of the machine does not create a serious issue due to high inertia of the machine. The effect of the slip on the torque is shown in Fig. 14. It can be observed that the torque of the machine increases with slip. However, a frequency of 65 Hz (slip: 0.18) is chosen for the analysis, since it provides the

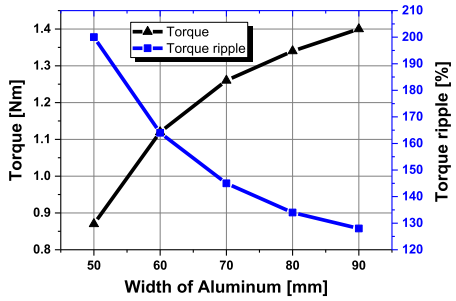

FIGURE 12. Effect of aluminum width on torque.

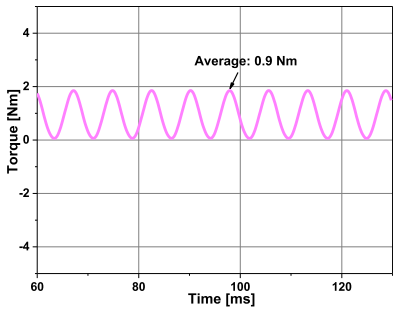

FIGURE 13. Simulated output torque.

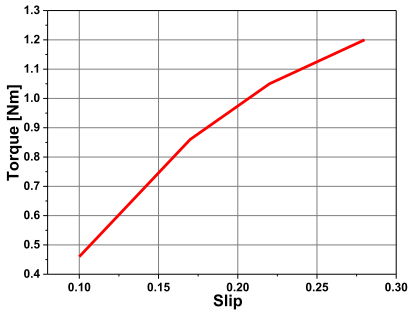

FIGURE 14. Effect of slip on torque.

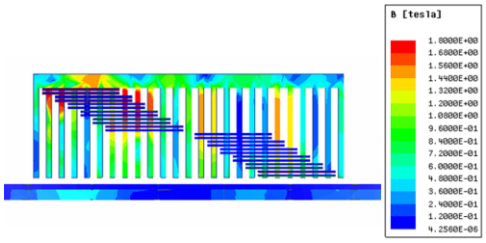

FIGURE 15. Flux density.

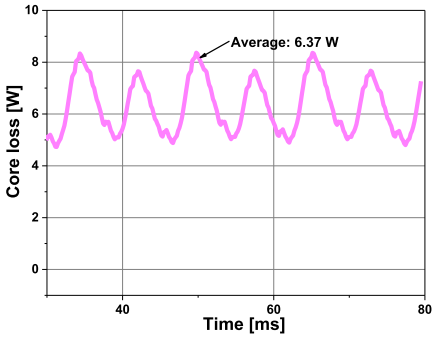

FIGURE 16. Core losses.

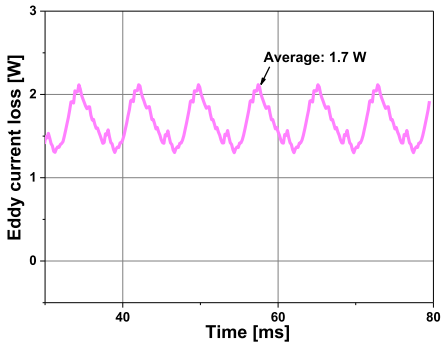

FIGURE 17. Eddy current losses.

required torque to rotate the REB at the desired speed. The flux density of the machine is shown in Fig. 15, where the M-LIM is working under the saturation limit.

The losses of the machine are calculated to determine the efficiency of the machine. The resistance/phase of the winding was measured, and the copper losses were calculated. The copper losses of the machine were found to be 38 W. The copper losses were high due to high resistance of the winding, which reduces the efficiency of the machine drastically. At 65 Hz armature current frequency and rated current, the core losses of the machine were calculated using FEM and are shown in Fig. 16. In stable state, the average core losses were found to be 6.37 W. The eddy current losses of the secondary are shown in Fig. 17.

The average eddy current losses were found to be 1.7 W. Based on these losses and the output power of the machine, the efficiency of the machine was found to be 27 %. The main reason for low efficiency is high copper losses. Owing to the limited stack length of the machine, the end winding length is also high. Moreover, the output power of the machine is also low. All these factors contribute to low efficiency of the machine. However, the efficiency of the machine can be improved by optimizing different factors and specially reducing the end winding length of the machine.

B. EXPERIMENTAL VALIDATION OF MODULAR LIM

Based on the 3-D FEA results, a prototype of the machine with the complete REB system is constructed. Considering the outer and inner diameters of the REB, as well as the required thrust force, two modules of primary are installed. The experimental setup of the machine is shown in Fig. 18. It is evident that the inner part of the REB is hollow indicating that it can be installed around a pillar. The two primary modules facing downwards (one primary module is visible in the picture) are installed on the top. Just below the primary modules, the ring-shaped aluminum plate of the secondary is installed. Its width (excluding the bearing) is the same as the REB width. Below the aluminum plate,

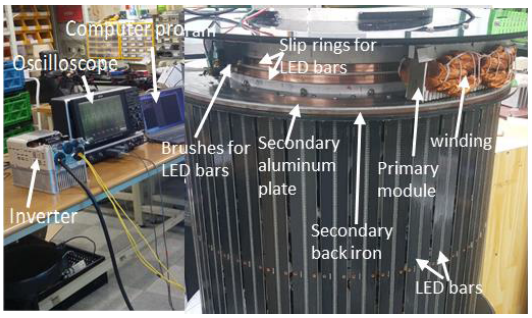

FIGURE 18. Experimental setup (prototype of the REB including M-LIM).

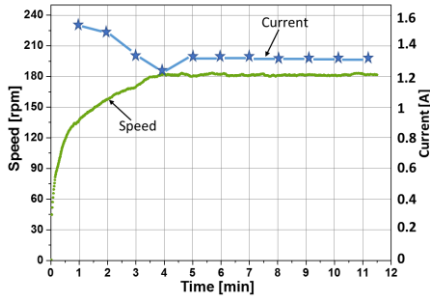

FIGURE 19. Measured speed/ currents.

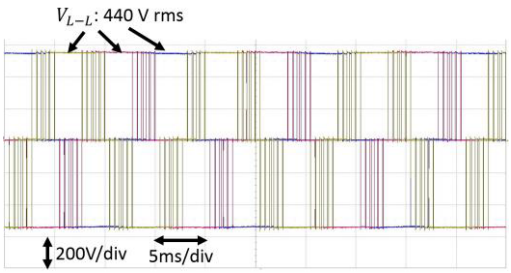

FIGURE 20. Measured line to line voltages.

the secondary back iron is installed and is in turn attached to the LED bars such that the LED bars rotate along with the secondary. A small speed sensor is installed at the back side of the LED bars, which is programmed to send signals to a computer program through Wi-Fi. Using this sensor, the rotating speed of the machine is measured. The machine is driven using a commercial inverter (Yaskawa A1000). The inverter supplies the required voltages to the two primary modules which exert the force on the secondary and thereby rotating the secondary along with the LED bars. The measured rotating speed of the LED bars is shown in Fig. 19.

The machine is driven using the V/f control scheme. The machine is started with the voltages having 60 Hz frequency. The machine reaches 140 rpm at this frequency. To increase the speed, the frequency is increased in increments of 5 Hz until the machine reaches the required speed of 180 rpm; however, the thrust force required for 180 rpm is obtained at 65 Hz. Due to the slow induction, this thrust force becomes

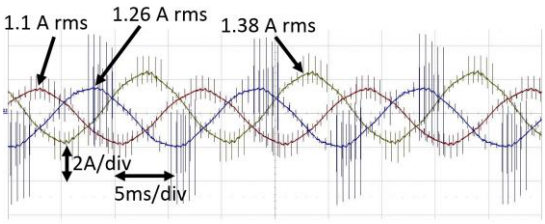

FIGURE 21. Measured currents.

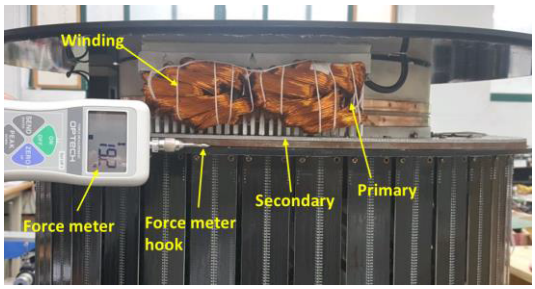

FIGURE 22. Force measurement setup.

stable after some time; therefore, after around 4 min, the frequency of the machine is slowly decreased to achieve a stable speed of 180 rpm. The rotating speed of the machine at 65 Hz remains in the range of 180-184 rpm, which is within the allowed range for LED bar with a frame rate of 180 Hz. When the machine is started at 60 Hz, it draws a large amount of current owing to the high inertia of the load. As can be seen from Fig. 19, when the frequency of the machine is increased, it draws less current; however, as the force of the machine increases with higher frequency, the rotating speed of the LED bar also increases. At 65 Hz, the machine draws a fixed amount of current that in turn provides a constant thrust force and constant rotating speed for the LED bars.

Since, the required rotating speed of the machine is achieved at 65 Hz, the simulation results and experimental results are compared at this frequency. The measured line-to-line voltages (three-phase) are shown in Fig. 20, where each phase has an rms value of 440 V, which is the same as the simulated condition. Each horizontal division corresponds to 5 ms and each vertical division corresponds to 200 V. The corresponding currents are shown in Fig. 21, where each horizontal division corresponds to 5ms and each vertical division corresponds to 2 A. It can be seen that the 3-phase currents are unbalanced (similar to simulation) with rms values of 1.1, 1.26 and 1.38 A. The 3-D measured currents show good agreement with simulated values, and the difference is attributable to the manufacturing tolerances of the machine and the other REB system components.

Since, there is no shaft in the built REB system, the torque cannot be measured. Alternatively, force is measured to verify the designed machine. A setup was specially built to measure the peak starting thrust force of the machine at locked rotor condition. A setup as shown in Fig. 22 is specially built to measure the peak starting thrust force of the machine at

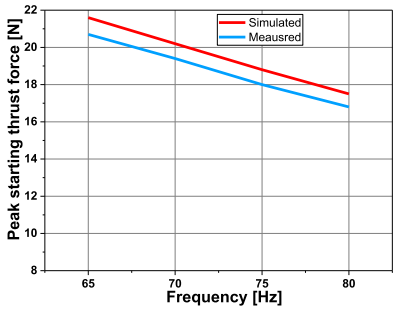

FIGURE 23. Comparison of peak starting thrust force (locked rotor).

FIGURE 24. LED display (180 rpm).

TABLE 3. Comparison of 3-D and experiment results.

Item	Unit	3-D	Experiment
Input voltage (Line to line)	V	440	
Current (rms)	A	1.29	1.29
X- Force	N	3	-
Peak Starting thrust force	N	21.8	20.8

locked rotor condition. A commercial force meter (OPTECH) company is used to hold the rotor by the hook. The voltages of the inverter are limited such that the machine cannot draw more current than the rated values. The force meter records the peak starting thrust force, when the voltages are applied. It should be noted that the force meter is held in such a manner that the tangential force is measured; however, considering the human error in holding the force meter tangent to the ring-shaped secondary, the experiment is repeated ten times and an average value of the peak force is taken to minimize the error as much as possible. The comparison of the measured and simulated values of the peak starting thrust force is shown in Fig. 23. An error of around 4.5% is found between the simulated and measured values. This is caused by the manufacturing tolerances and the human error in holding the force meter in tangent direction. The comparison of 3-D and experimental results is shown in Table 3.

The measured voltages, currents, speed, and starting thrust force of the machine confirm that the designed machine achieves the desired rotating speed for the LED bars. The LED display for rotating speed of 180 rpm and a frame rate of 180 Hz is shown in Fig. 24, which confirms that the designed M-LIM fulfills the requirements of REB as envisaged in this study.

V. CONCLUSION

This paper proposed a rotating electronic billboard (REB) to save the cost of space required for its installation and a modular linear induction machine (M-LIM) to rotate the proposed REB. A modular LIM with a short primary and ring-shaped secondary was designed and to rotate the proposed REB. A prototype of the M-LIM along with the complete proposed REB setup was manufactured and experiments were performed. The experimental results showed good agreement with simulation. The REB was rotated using the designed M-LIM, the videos/advertisements were displayed, and the overall performance was found to be satisfactory, confirming that REB is a promising application for the M-LIMs.

A single primary module could be commonly used for all sizes of REBs. The number of primary modules could be varied according to the size of the REB. Moreover, the proposed M-LIM required less space than the rotary machines. Consequently, the complete REB system occupied less space because it could be installed around the pillars, that, in contrast, was a drawback of the conventional REBs. Hence, the cost of the space required for installing REBs is also limited. The proposed modular design can be used in other applications such as low speed MAGLEV and circular moving platform for pedestrian walking. It is worth mentioning that other machines such as synchronous reluctance machines and switched reluctance machines can also be used with modular structure in the proposed REB, which will have higher efficiency. However, since they are not line-start machines, therefore an inverter will be mandatory which will increase the cost of the system which is undesirable for commercialization. Furthermore, the overall system cost and size of the proposed REB could be higher compared to commercial conventional REB [27], however, the proposed REB requires less space cost and lower initial development costs for different sizes of REBs owing to its modular structure.

REFERENCES

[1] J.-H. Choi, J.-S. Kim, and K.-H. Kim, "Robust tracking performance of linear induction motor-based automatic picking system using a high-gain disturbance observer," *IET Electr. Power Appl.*, vol. 10, no. 1, pp. 45–53, Jan. 2016.

[2] J.-Q. Li, W.-L. Li, G.-Q. Deng, and Z. Ming, "Continuous-behavior and discrete-time combined control for linear induction motor-based urban rail transit," *IEEE Trans. Magn.*, vol. 52, no. 7, Jul. 2016, Art. no. 8500104.

[3] M. Flankl, L. de Oliveira Baumann, A. Tüysüz, and J. W. Kolar, "Energy harvesting with single-sided linear induction machines featuring secondary conductive coating," *IEEE Trans. Ind. Electron.*, vol. 66, no. 6, pp. 4880–4890, Jun. 2019.

[4] J. Di, Y. Fan, Y. Liu, S. Liu, and Y. Zhu, "Variable pole pitch electromagnetic propulsion with ladder-slot-secondary double-sided linear induction motors," *Appl. Sci.*, vol. 7, no. 5, p. 481, 2017.

[5] Y. Zhang, M. Zhang, W. Ma, J. Xu, J. Lu, and Z. Sun, "Modeling of a double-stator linear induction motor," *IEEE Trans. Energy Convers.*, vol. 27, no. 3, pp. 572–579, Sep. 2012. doi: 10.1109/TEC.2012.2197622.

[6] A. Musolino, M. Raugi, R. Rizzo, and M. Tucci, "Force optimization of a double-sided tubular linear induction motor," *IEEE Trans. Magn.*, vol. 50, no. 12, Dec. 2014, Art. no. 8206911. doi: 10.1109/TMAG.2014.2343591.
[7] Y. Nozaki, J. Baba, K. Shutoh, and E. Masada, "Improvement of transverse flux linear induction motors performances with third order harmonics current injection," *IEEE Trans. Appl. Supercond.*, vol. 14, no. 2, pp. 1846–1849, Jun. 2004. doi: 10.1109/TASC.2004.830880.
[8] W. Xu, G. Sun, G. Wen, Z. Wu, and P. K. Chu, "Equivalent circuit derivation and performance analysis of a single-sided linear induction motor based on the winding function theory," *IEEE Trans. Veh. Technol.*, vol. 61, no. 4, pp. 1515–1525, May 2012. doi: 10.1109/TVT.2012.2183626.
[9] V. Ahmad, G. V. Sadler, and A. W. Davey, "Applications of linear induction motors in industry," *Proc. Inst. Elect. Eng.*, vol. 119, no. 2, pp. 233–234, Feb. 1972. doi: 10.1049/piee.1972.0046.
[10] J. Han, Y. Du, Y. Li, N. Jin, T. Zhou, and W. Xu, "Study and optimized design of stator core structure in single-sided linear induction motor," in *Proc. Int. Conf. Elect. Mach. Syst.*, Wuhan, China, Oct. 2008, pp. 3464–3469.
[11] B. Laporte, N. Takorabet, and G. Vinsard, "An approach to optimize winding design in linear induction motors," *IEEE Trans. Magn.*, vol. 33, no. 2, pp. 1844–1847, Mar. 1997. doi: 10.1109/20.582640.
[12] M. H. Ravanji and Z. Nasiri-Gheidari, "Design optimization of a ladder secondary single-sided linear induction motor for improved performance," *IEEE Trans. Energy Convers.*, vol. 30, no. 4, pp. 1595–1603, Dec. 2015. doi: 10.1109/TEC.2015.2461434.
[13] A. H. Isfahani, B. M. Ebrahimi, and H. Lesani, "Design optimization of a low-speed single-sided linear induction motor for improved efficiency and power factor," *IEEE Trans. Magn.*, vol. 44, no. 2, pp. 266–272, Feb. 2008. doi: 10.1109/TMAG.2007.912646.
[14] A. Z. Bazghaleh, M. R. Naghashan, M. R. Meshkatoddini, and H. Mahmoudimanesh, "Optimum design of high speed single-sided linear induction motor to obtain best performance," in *Proc. SPEEDAM*, Pisa, Italy, Jun. 2010, pp. 1222–1226.
[15] S. Nonaka and T. Higuchi, "Design of single-sided linear induction motors for urban transit," *IEEE Trans. Veh. Technol.*, vol. 37, no. 3, pp. 167–173, Aug. 1988. doi: 10.1109/25.16543.
[16] G. E. Dawson, A. R. Eastham, J. F. Gieras, R. Ong, and K. Ananthasivam, "Design of linear induction drives by field analysis and finite-element techniques," *IEEE Trans. Ind. Appl.*, vol. IA-22, no. 5, pp. 865–873, Sep. 1986. doi: 10.1109/TIA.1986.4504805.
[17] J. Atencia, A. G. Rico, and J. Flórez, "A low cost linear induction motor for laboratory experiments," *Int. J. Elect. Eng. Educ.*, vol. 38, no. 2, pp. 117–134, 2001.
[18] R. Hofmann, A. Binder, and R. Pfeiffer, "Investigations on a linear induction machine for railway applications," in *Proc. IEEE Int. Electr. Mach. Drives Conf. (IEMDC)*, Cambridge, MA, USA, Jun. 2001, pp. 20–26. doi: 10.1109/IEMDC.2001.939267.
[19] G. Lv, Z. Liu, and S. Sun, "Analysis of torques in single-side linear induction motor with transverse asymmetry for linear metro," *IEEE Trans. Energy Convers.*, vol. 31, no. 1, pp. 165–173, Mar. 2016.
[20] B. Liu, X. Zhang, and J. Fang, "A novel secondary structure to research on dynamic longitudinal edge effect of a short-primary HTS linear induction motor for subway transportation," *IEEE Trans. Appl. Supercond.*, vol. 26, no. 7, Oct. 2016, Art. no. 5207305.
[21] B. Jandaghi and V. Dinavahi, "Hardware-in-the-loop emulation of linear induction motor drive for maglev application," *IEEE Trans. Plasma Sci.*, vol. 44, no. 4, pp. 679–686, Apr. 2016.
[22] I. Takahashi and Y. Ide, "Decoupling control of thrust and attractive force of a LIM using a space vector control inverter," *IEEE Trans. Ind. Appl.*, vol. 29, no. 1, pp. 161–167, Jan. 1993.
[23] I. Boldea, L. N. Tutelea, W. Xu, and M. Pucci, "Linear electric machines, drives, and MAGLEVs: An overview," *IEEE Trans. Ind. Electron.*, vol. 65, no. 9, pp. 7504–7515, Sep. 2018.
[24] C. R. Taylor, G. R. Franke, and H.-K. Bang, "Use and effectiveness of billboards: Perspectives from selective-perception theory and retail-gravity models," *J. Advertising*, vol. 35, no. 4, pp. 21–34, 2006.
[25] *Rectangular Electronic Billboard Advertisement (Korean)*. Accessed: Feb. 2018. [Online]. Available: http://blog.daum.net/assalys/10
[26] B. Jones and G. Spector, "Electronic billboard," U.S. Patent 5 257 017 A, Oct. 10, 1993.
[27] *Rotating Electronic Billboards*. Accessed: Feb. 2018. [Online]. Available: http://www.dynascanusa.com/products/360-degree-led-video-displays/
[28] H. J. Dehli, "Advertising display apparatus with precise rotary drive," U.S. Patent 5 513 458 A, May 7, 1996.
[29] J. F. Gieras, *Linear Induction Drives*, vol. 30. London, U.K.: Oxford Univ. Press, 1994.
[30] J. Lu and W. Ma, "Investigation of phase unbalance characteristics in the linear induction coil launcher," *IEEE Trans. Plasma Sci.*, vol. 39, no. 1, pp. 110–115, Jan. 2011.

NOMAN BALOCH received the B.S. degree in electronics engineering from the Balochistan University of Information Technology, Engineering and Management Sciences (BUITEMS), Quetta, Pakistan, in 2010. He is currently pursuing the M.S. leading to Ph.D. degree with the Department of Electronics System Engineering, Hanyang University, Ansan, South Korea.

From 2010 to 2015, he was the Deputy Assistant Director with the National Database and Registration Authority (NADRA), Pakistan. His research interest includes design and control of electrical machines.

CHA-SEUNG JUN was born in 1972. He received the B.S. and M.S. degrees in electrical engineering and the Ph.D. degree in electronic systems engineering from Hanyang University, Ansan, South Korea, in 1996, 1998, and 2017, respectively. From 1999 to 2000, he was a Research Engineer with Delco Remy Korea, Ltd. Since 2000, he has been a Research Engineer and the Project Manager with LG Electronics Inc., where he has performed lots of projects on design and control of electric motors for home appliance. His current research interest includes design and control of electric motors.

BYUNG-IL KWON was born in 1956. He received the B.S. and M.S. degrees in electrical engineering from Hanyang University, Ansan, South Korea, in 1981 and 1983, respectively, and the Ph.D. degree in electrical engineering, machine analysis from the University of Tokyo, Tokyo, Japan, in 1989.

From 1989 to 2000, he was a Visiting Researcher with the Faculty Member of Science and Engineering Laboratory, University of Waseda, Tokyo, Japan. In 1990, he was a Researcher with the Toshiba System Laboratory, Yokohama, Japan. In 1991, he was a Senior Researcher with the Institute of Machinery and Materials Magnetic Train Business, Daejeon, South Korea. From 2001 to 2008, he was a Visiting Professor with the University of Wisconsin–Madison, Madison, WI, USA. He is currently a Professor with Hanyang University. His research interest includes design and control of electric machines.